CALIBRATION OF GROUND WEATHER RADAR SYSTEMS FROM TRMM PRECIPITATION RADAR OBSERVATIONS: APPLICATION TO THE S-BAND RADAR IN BAURU, BRAZIL.

Emmanouil N. Anagnostou and Carlos A. Morales
Department of Civil and Environmental Engineering
University of Connecticut, Storrs, CT, USA

Roberto Vicente Calheiros
FET/IPMet
Universidade do Estado de Sao Paulo, Bauru, Brazil

Abstract

This research uses a newly developed methodology to evaluate ground weather radar (GR) calibration biases from coincident Tropical Rainfall Measuring Mission (TRMM) Precipitation Radar (PR) observations. The method matches GR and PR observations in a common earth parallel three-dimensional Cartesian grid. The data matching is performed in a way that minimizes uncertainties associated with the type of weather seen by the radars, grid resolution, and differences in radar sensitivities, sampling volumes, viewing angles, and radar frequencies. We present application of the method to the S-band Doppler Radar in Bauru, Brazil. Reflectivity difference statistics derived from the matched GR-PR data reveal systematic differences around 6 dB, which is attributed to GR calibration bias. Temporal analysis of the GR-PR systematic differences reveals fluctuations of less than 1 dB, which is around the calibration stability of the PR. The proposed scheme can be a useful tool to radar engineers for the systematic monitoring of their radar system calibration.

1. Introduction

Ground-based volume scanning weather radars can provide rainfall observations at spatio-temporal scales suitable for applications varying from hydrologic forecasting to climate monitoring. However, the lack of accurate determination of the radar calibration constant (hereafter referred as radar calibration bias) can be a significant error source to the quantitative interpretation of radar measurements. Smith et al. (1996) has shown that this error can cause significant radar-to-radar rainfall observation differences, and should be quality controlled before applying any rainfall estimation algorithm. Ulbrich et al. (1999) in a sensitivity study of the Z-R relationship also underscored the need for absolute calibration of ground-based radars. For getting the exact radar constant field test using either metal spheres or active sources of radiation are required, which are labor-intensive processes and therefore quite infrequent. Currently, the problem of radar calibration bias has been addressed jointly with other systematic error sources through procedures that apply to radar-rain gauge rainfall accumulation comparisons (Anagnostou et al., 1998a; Smith and Krajewski, 1991). However, these comparisons, due to the large difference in the sampling geometry of the two sensors and the high variability of the Z-R relationship, are noisy and difficult to interpret (Anagnostou et al., 1999; Kitchen and Blackall, 1992).

In this paper we attempt to address the problem of radar calibration bias adjustment using observations from the first space-based radar (PR) aboard the recently launched Tropical Rainfall Measuring Mission (TRMM) satellite (Simpson et. al, 1996). The PR, which has an attenuated frequency (13.8 GHz) and a nominal sensitivity threshold of about 17 dBZ, has been demonstrated by the National Space and Development Agency of Japan (NASDA) to be consistent with calibration stability within 0.8 dB (Kozu et al., 2000; Kawanishi et al., 1998, 2000). A newly developed methodology (Anagnostou et al., 2000) is used to match PR and GR observations leading to the determination of calibration biases in GR systems. We base this investigation on the fact that PR and GR systems measure the same variable (i.e., reflectivity), and that PR is fairly consistent with respect to calibration accuracy. We used several storm cases of coincident PR and GR data from the Bauru S-band radar site in Brazil to demonstrate the method. It is shown that PR observations can be used to systematically monitor the calibration coefficient of the GR system.

In the following section we provide background information on the methodology used to match PR and GR measurements. In section 3 we present the case study, while in Section 4 we offer our conclusions and discussion for future research.

2. Background

A methodology has been developed with goal the estimation of systematic errors in GR reflectivity measurements by comparing against coincident PR observations. The method is based on a scheme that interpolates ground and space radar volume scans into a fixed grid, and a data selection that minimizes uncertainties associated with the issues described above. The interpolation scheme and data selection is described next.

Instantaneous PR and GR reflectivity volume scans that are within a maximum of 3-minutes time lag are projected into a common earth-parallel three-dimensional Cartesian grid (hereafter called 3D-box) with 5-km×5-km horizontal and 2-km vertical resolution. The 3D-box pixel dimensions are selected to be consistent with both the GR's low vertical resolution (~2 km at 100 km range for 1° beam width) and the PR's field-of-view resolution (~4.5-km × 4.5-km). The 3D-box is centered at each GR site with horizontal extent of ±100 km, and vertical levels ranging from a minimum of 2-km to a maximum of 12-km. Below 2-km both PR and GR data may be contaminated by ground returns, while above 10-km the gaps in upper elevation sweeps of GRs may introduce significant interpolation errors. The actual lower and upper levels of each pixel within the 3D-box grid are variable and depend on the elevation of the zero isotherm and the highest elevation with detectable (>18 dBZ) PR reflectivity. Each ray of a PR swath is projected on the 3D-box using information about the spacecraft location and altitude (from satellite navigation algorithm), the beam inclination, and a stereographic projection scheme. The projected PR reflectivity values (mm^6m^{-3}) are subsequently averaged in the vertical to produce the 3D-box pixel values.

The GR reflectivity volume scans are transformed from polar coordinates to the 3D-box through conversion tables. These tables indicate the radar polar samples, and relative weights representing their volume fraction, that correspond to each 3D-box pixel. They are constructed using an algorithm that simulates the radar sampling process (Anagnostou and Krajewski, 1997) accounting for beam propagation, refraction, and widening, according to a specified radar sampling geometry and mean refractive index profile (Battan, 1973). Refractive index profiles are determined based on the nearest in time and space atmospheric sounding data, or in a more simplified form using the $4/3^{rd}$ earth radius model of the refractive index profile (Doviac and Zrnic, 1993). Since the radar sampling (elevation sweeps, azimuth and range samples, etc.) may vary from scan-to-scan a fixed polar grid is defined where radar volume scans are projected. The fixed polar grid resolution is based on the radar sampling specifications, namely beam-width, range averaging, and elevation angles. The interpolation of the variable polar radar samples to the fixed polar grid is based on the square-inverse distance method. In this study the fixed polar grid is defined at polar cells of 1-degree azimuth and 1-km range resolution, and 1-degree elevation increments.

Although, the above matching scheme can minimize uncertainties associated with the sampling resolution differences of the two radars, additional steps are needed to make the PR-GR comparisons meaningful for the purpose of identification of GR calibration biases. The steps are (1) attenuation correction of the raw PR reflectivity profiles; (2) classification of precipitation systems to convective, stratiform and mixed type; (3) determination of the bright band (mixed phased hydrometeors) level; and (4) definition of the lower and upper levels for each 5-km×5-km vertical column of the 3D-box. The method uses attenuation corrected PR reflectivity values retrieved from the TRMM Science Data and Information System (TSDIS) 2A-25 algorithm (Simpson et al., 1996) documented in Iguchi and Meneghini (1994). The algorithm, which combines the iterative scheme of Hiltschfeld-Bordan with a surface reference method, has been shown using TRMM data that can offer great attenuation correction accuracy (Iguchi et al., 2000). The precipitation classification and bright band level determination are two products provided by the TSDIS 2A-23 algorithm, which is based on algorithms described in Iguchi et al. (2000). The lower level for each grid in the 3D-box is defined as the level of the first pixel above the bright band, while the upper level is the upper most pixel level where all PR samples that contribute to the pixel average exceed the 18-dBZ threshold. We eliminate sections of the 3D-box that are classified as mainly convective. This serves to the reduction of uncertainty due to the high sub-grid precipitation variability associated with these systems and random effects due to changes of precipitation type. Furthermore, constraining the analysis above the bright band and to mainly stratiform systems eliminates uncertainties associated with attenuation correction errors. Finally, the viewing angle and signal frequency (non-Rayleigh effect) differences between space and ground radars are minor issues when considering frozen phase hydrometeors (ice, snow, etc.).

The final step of our methodology is evaluation of the systematic difference between the PR and ground radar data. Two methods are applied to the selected 3D-box matched reflectivity values. The first method is based on the sample statistics of the reflectivity differences (in dB), namely the mean (B_{smp}) and standard deviation (σ_{smp}):

$$B_{smp} = \frac{1}{n}\sum_{n}(Z_{GR} - Z_{PR}) \quad (1)$$

$$s_{smp}^{2} = \frac{1}{n}\sum_{n}(Z_{GR} - Z_{PR})^{2} - B_{smp}^{2} \quad (2)$$

where Z_{GR} and Z_{PR} are the selected 3D-box matched reflectivity values (in dBZ) of the ground radar and PR, respectively, and n is the sample size. The standard deviation of the difference is used to derive the confidence interval (L) for the estimated mean difference (B_{smp}):

$$L = \pm t_a \frac{s_{smp}}{\sqrt{n}} \quad (3)$$

where t_a is the a^{th} quantile point of the t distribution with n degrees of freedom.

The second method evaluates the bias coefficient (B_{pdf}) that minimizes an objective function (f) that measures the square difference between the frequency distributions of the two matched radar data. The objective function is defined as:

$$f(B_{pdf}) = \frac{1}{n_1}\sum_{i=1}^{n_1}\left(\left[f_{GR}(Z_i \cdot B_{pdf}) - f_{PR}(Z_i)\right]\cdot Z_i\right)^{2} \quad (4)$$

where f_{GR} and f_{PR} are the jumps of ground radar and PR reflectivity step cumulative density functions at discrete values Z_i, and n_1 is the number of these discrete steps. It is noted that estimation of B_{pdf} with this method is subject to significant uncertainty for small sample sizes (<100).

3. Case Study

A procedure is used that based on TRMM satellite navigation information and TRMM rainfall products identifies overpasses with significant coincident precipitation coverage within 100-km radar radius of a specified ground radar site. In this study we concentrated on the S-band Doppler weather radar site in Bauru, Brazil (**lat and lon info**). We selected cases with common precipitation coverage larger than 20% for a period ranging from 1997 to the end of 1999.

Figure 1 shows an example of horizontal reflectivity distributions (at 2-km level, CAPPI) and reflectivity cross-section profiles of the PR and GR for a case (13 January 1999) with significant precipitation coverage in the overlapping area of the two radars. The figure has six panels. The upper three panels show the 2-km CAPPI and two cross-sections of the PR attenuation corrected data (2A-25). The lower three panels show the same plots but for the coincident GR data. The radar circles shown in the figure have 150-km radius. One can note that although the patterns and positioning of the systems are the same for both radars there is significant difference in the relative magnitude of their corresponding values. The cross-correlation between PR and GR is about 0.82 for zero space-lag, and drops rapidly below 0.7 for lags greater than one. One can also note the higher sensitivity of the GR with respect to the PR, which does not see reflectivity values lower than 17 dBZ. This issue is addressed in our methodology by excluding these PR pixels from the analysis.

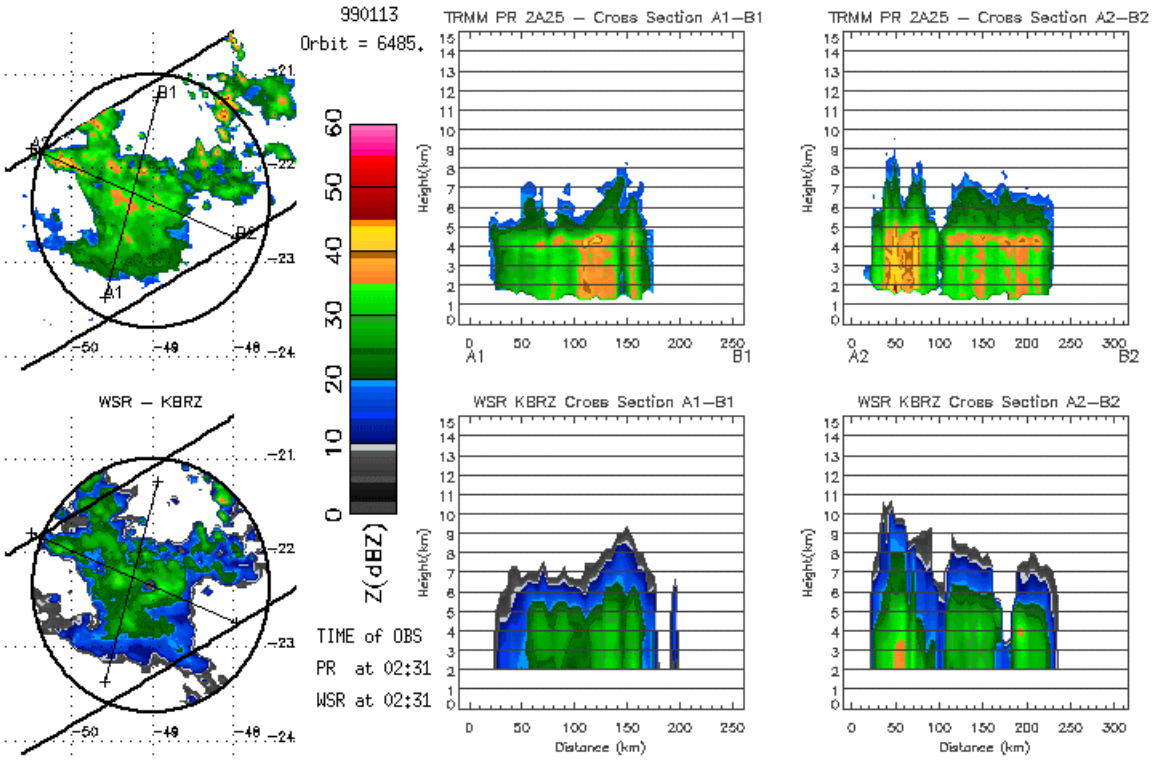

Figure 1: Comparison of reflectivity fields at 2-km CAPPI and two vertical cross sections from the attenuation corrected PR (2A-25) and the Bauru GR for the 13 January 1999 matched case. The circles correspond to 150 km radar ranges.

A quantitative comparison between PR and GR is described next. Figure 2 (upper left panel) shows the GR-PR reflectivity difference (in dB) histogram associated with the selected cases. A first observation extracted from this panel is that the histogram has Gaussian shape. The standard deviation is 2.5 dB. This variability is attributed to random effects associated with the hydrometeors size distribution variability, residual attenuation correction errors, incomplete knowledge of the ground radar beam propagation, ground radar interpolation errors due to gaps in their elevation sweeps (up to 4 degrees), and temporal lags (up to 3 minutes) between PR and GR measurements. Nevertheless, one can clearly distinguish the significant systematic difference between the two sensor measurements. The upper right panel of Figure 2 shows scatter plot of the PR reflectivity versus reflectivity difference values of the matched 3D-box data. It is apparent that there is no obvious dependence of the difference on the reflectivity magnitude. The reflectivity values are less than 40 dBZ, which is a result of the constraints posed by our methodology in the selection of the matched 3D-box data. Furthermore, classification of the reflectivity differences with respect to the level above the bright band has shown no obvious dependence. These two observations support the use of a fixed multiplicative coefficient, which is evaluated from the matched dataset according to equations (1) or (4), and applied uniformly to the whole ground radar measurements. Finally, the lower panel of Figure 2 shows time series of the Bauru GR bias (in dB) estimated using our proposed methodology. The horizontal axis of this panel shows the dates of the matched datasets used in the bias estimates. The vertical bars plotted for each bias estimate represent its 95% confidence intervals evaluated using equation (3). These bounds represent the range of uncertainty of the estimated ground radar bias, which is function of the sample size used in the estimation and the reflectivity difference variance. The two horizontal lines correspond to the overall bias estimates derived from our two methods, namely the sample mean (red line) and the probability distribution matching (blue line). It is shown that the temporal fluctuation of the bias is less than 1 dB, which is within the calibration accuracy of the PR system. Furthermore, is shown that the bias estimates derived from the two methods are the same, which statistically verifies the observation that the reflectivity differences have Gaussian distribution.

4. Conclusions

A methodology that matches PR and GR measurements in a common earth parallel three-dimensional grid was used in this study to evaluate the calibration bias of an S-band weather radar located in Bauru, Brazil. The

methodology uses satellite navigation information, a radar sampling geometry model accounting for ray propagation under vertically stratified refractive index, and polar-stereographic projection to interpolate PR and GR data in the fixed 3D-box. We demonstrated good matching between GR and PR reflectivity patterns, with correlations at levels above the bright band varying from 0.8 to 0.95. Evaluation of the difference statistics revealed significant systematic difference (-6 dB), which is attributed mainly to GR calibration bias. It was concluded that the bias has not obvious dependence on the reflectivity magnitude neither on altitude. The temporal fluctuation of the radar bias was not significant (< 1dB).

We are expanding the applications of our method to several radar sites including the WSR-88Ds in the USA, as well as other international sites. The current compiled database may be viewed at the World Wide Web (http://www.engr.uconn.edu/~gracp). The methodology provides an attractive framework for routine monitoring of ground radar system calibration biases over the globe, using as reference the stable PR measurements.

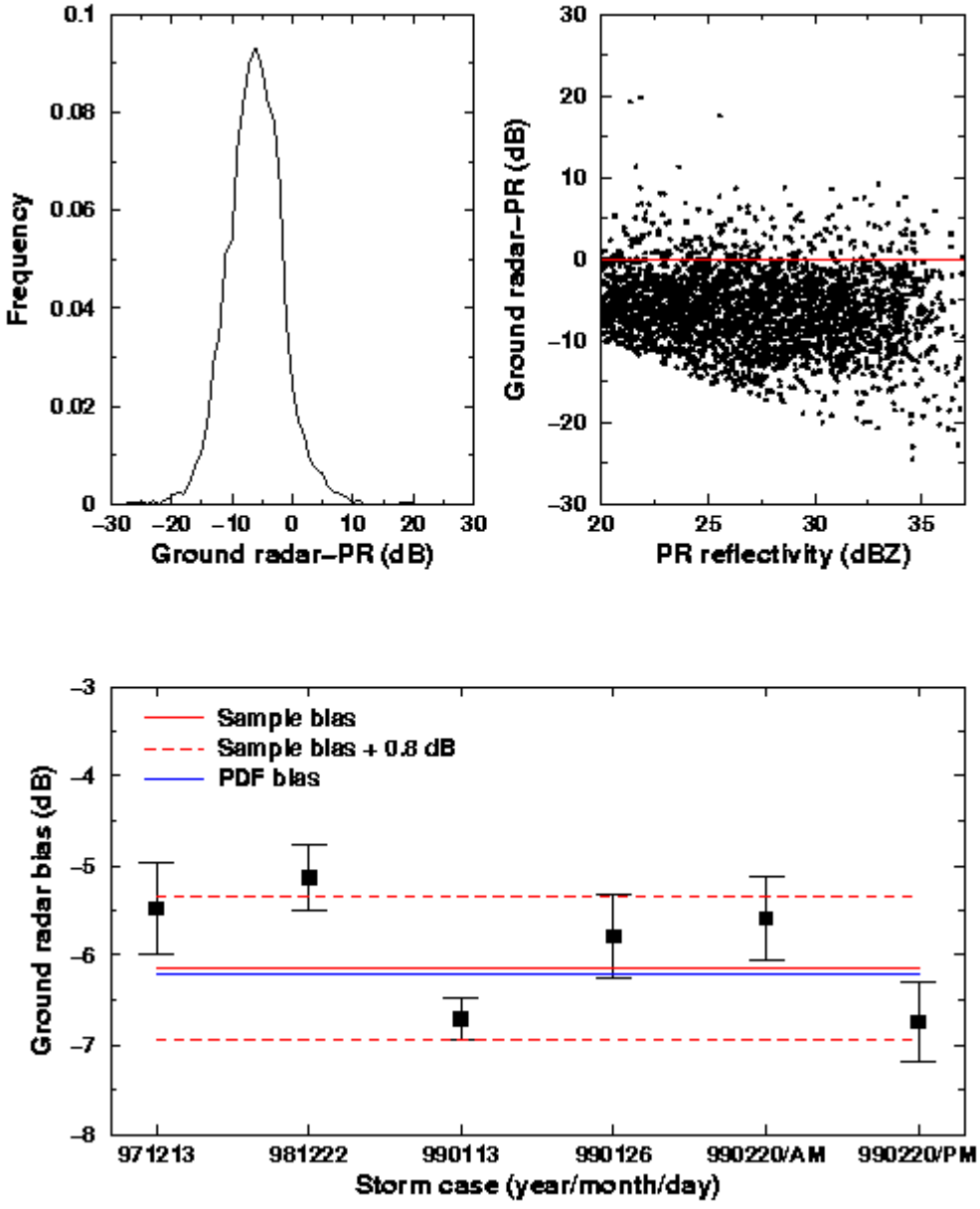

Figure 2: Upper left panel: Histogram of GR-PR differences (in dB). Upper right panel: Scatter plot of GR-PR difference versus PR reflectivity value. Lower panel: Time series of GR bias estimated based on our method.

5. References:

Anagnostou E.N., C. Morales, and T. Dinku (2000). “On the Use of TRMM Precipitation Radar Observations in Determining Ground Radar Calibration Biases,” Submitted to *J. of Atmos. and Ocean. Technology*.

Anagnostou, E.N., and W.F. Krajewski (1997). “Simulation of Radar Reflectivity Fields: Algorithm Formulation and Evaluation,” *Water Resources Research*, 33(6), 1419-28.

Anagnostou, E.N., W.F. Krajewski, D.-J., Seo, and E.R., Johnson (1998a). "Mean-field radar rainfall bias studies for NEXRAD." *ASCE J. of Hydrol. Engin.*, 3(3), 149-159.

Anagnostou, E.N., and W.F. Krajewski (1998b). "Calibration of the WSR-88D Precipitation Processing Subsystem." *Weather and Forecasting*, 13, 396-406.

Anagnostou, E.N., W.F. Krajewski, and J. Smith, (1999). "Uncertainty Quantification of Mean-Field Radar-Rainfall Estimates," *Journal of Atmospheric and Oceanic Technology*, 16, 206-215.

Battan, L.J.. *Radar Observation of the Atmosphere*. The University of Chicago Press, 1973.

Doviak, R.J. and D.S., Zrnic, (1993). “*Doppler Radar and Weather Observations*,” 2nd edition, Academic Press Inc., Orlando, Florida.

Iguchi T, Meneghini R, Awaka J, Kozu T, Okamoto K (2000). “Rain profiling algorithm for TRMM precipitation radar data,” *Remote Sensing and Applications: Earth, Atmosphere and Oceans*, 25(5), 973-976.

Iguchi T, and Meneghini R (1994). “Intercomparison of Single-Frequency Methods for Retrieving a Vertical Rain Profile from Airborne or Spaceborne radar data,” *J. Atmos. Ocean. Techn*., 11(6), 1507-1516.

Kawanishi, T., T. Kozu, R. Meneghini, J. Awaka, and K. Okamoto (1998). "Preliminary results of rain profiling with TRMM precipitation radar." Proc. *SPIE: Microwave Remote Sensing of the Atmosphere and Environment*, Beijing, China, 94-101.

Kitchen, M., and R.M. Blackall (1992). "Representativeness errors in comparisons between radar and gauge measurements of rainfall." *J. Hydrol.*, **134**, 13-33.

Kozu, T., T. Kawanishi, H. Kuroiwa, M. Kojima, K. Oikawa, H. Kumagai, K. Okamoto, M. Okumura, H. Nakatsuka, and K. Nishikawa (2000). “Development of Precipitation Radar Onboard the Tropical Rainfall Measuring Mission (TRMM) Satellite, *IEEE Trans. Geosciences and Remote Sensing* (accepted).

Kumagai, H., T. Kozu, M. Satake, H. Hanado and K. Okamoto (1995). “Development of an active radar calibrator for the TRMM precipitation radar,” *IEEE Trans. Geosci. Remote Sens.*, GE-33, 1316-1318.

Simpson J., C. Kummerow, W.-K. Tao, and R.F. Adler (1996). “On the Tropical Rainfall Measuring Mission (TRMM).” *Meteorol. Atmos. Phys*., 60, 19-36.

Smith, J.A. and W.F. Krajewski (1991). “Estimation of the Mean Field Bias of Radar Rainfall Estimates,” *Journal of Applied Meteorology*, 30(4), 397-412.

Smith, J.A., D.-J., Seo, M.L., Baeck, and M.D., Hudlow (1996). "An intercomparison study of NEXRAD precipitation estimates." *Wat. Resour. Res.* 32(7), 2035-2045.

Ulbrich, C. W., L. G. Lee (1999). “Rainfall Measurement Error by WSR-88D Radars due to Variations in Z–R Law Parameters and the Radar Constant”, *Journal of Atmospheric and Oceanic Technology*, Vol. 16, No. 8, pp. 1017–1024.